

**FÖRSTER RESONANCE ENERGY TRANSFER AND  
FLUORESCENCE QUENCHING BASED LOW-DENSITY  
LIPOPROTEIN PROBES FOR VISUALIZING TRANSCYTOSIS**

A Thesis  
Presented to  
The Academic Faculty

by

Nicole C. Fay

In Partial Fulfillment  
of the Requirements for the Degree  
B. S. Biology with Research Option & B. S. Biochemistry in the  
School of Biology & School of Chemistry and Biochemistry

Georgia Institute of Technology  
May 2008

COPYRIGHT 2008 BY NICOLE C. FAY

## **ACKNOWLEDGMENTS**

I wish to thank Dr. Christine K. Payne, Dr. John R. Kirby and all the associated lab members for mentoring my research and my interest in science.

# TABLE OF CONTENTS

	Page
ACKNOWLEDGMENTS	v
LIST OF FIGURES	viii
LIST OF SYMBOLS AND ABBREVIATIONS	ix
SUMMARY	x
<u>CHAPTER</u>	
1 INTRODUCTION	1
SIGNICANCE OF TRANSCYTOSIS	1
LOW-DENSITY LIPOPROTEIN AS AN IDEAL TRANSCYTIC CARGO	3
PRINCIPLES OF PROBE 1: FÖRSTER RESONANCE ENERGY TRANSFER	6
PRINCIPLES OF PROBE 2: FLUORESCENCE QUENCHING	7
MADIN-DARBY CANINE KIDNEY CELLS AS A MODEL CELL LINE FOR TRANSCYTOSIS	10
APPLICATIONS OF LDL PROBES	11
2 EXPERIMENTAL PROCEDURES	13
MATERIALS	13
FLUORESCENT LABELING OF LDL	14
DEGRADATION OF LDL PARTICLE VIA DETERGENT AND ENZYMES	14
VIZUALIZATION OF DIGEST VIA SDS-PAGE	15
SPECTROSCOPIC MEASUREMENTS	15
CELL CULTURE	16
DETERMINING MDCK POLARIZATION	17

TESTING QUENCHING PROBE <i>IN VIVO</i> BY FLOW CYTOMETRY	17
3 RESULTS	19
DETERMINING LDL CONCENTRATION	19
<i>IN VITRO</i> DETERGENT DEGRADATION OF LDL PROBES	19
<i>IN VITRO</i> ENZYMATIC DEGRADATION OF LDL PROBES	23
VISUALIZATION OF DEGRADATION VIA SDS-PAGE	23
TESTING IN LDL QUENCHING PROBE <i>IN VIVO</i> VIA FLOW CYTOMETRY	25
ASSAYING POLARIZATION OF MDCK MONOLAYER	26
4 DISCUSSION	29
5 CONCLUSION	31
REFERENCES	32

## LIST OF FIGURES

	Page
Figure 1: Transcytic Route versus Degradative Route of Intracellular LDL	5
Figure 2: Principles of FRET	8
Figure 3: Mechanism of LDL probe	9
Figure 4: LDL Absorbance at 271 nm	21
Figure 5: <i>In vitro</i> Detergent Degradation of Probes	22
Figure 6: <i>In vitro</i> Enzymatic Degradation of Probes	24
Figure 7: Visualization of FRET Probe Enzymatic Degradation via SDS-PAGE	25
Figure 8: MDCK TEER Values over Time	27
Figure 9: Images of Microtubule Reorganization after Polarization	28

## LIST OF SYMBOLS AND ABBREVIATIONS

$\epsilon$	Molar absorptivity or molar extinction coefficient ( $L * mol^{-1} * cm^{-1}$ )
LDL	Low-density lipoprotein
BBB	Blood brain barrier
MDCK	Madin-Darby canine kidney cells
FRET	Förster resonance energy transfer
DiI	1,1'- dioctadecyl - 3,3,3',3'-tetramethylin-docarbo-cyanine perchlorate
DiD	1,1'- dioctadecyl-3,3,3',3'- tetramethylin-dodicarbocyanine, 4-chlorobenzene-sulfonate salt
SDS-PAGE	Sodium dodecyl sulfate-polyacrylamide gel electrophoresis
TEER	Transepithelial Electrical Resistance
m	Milli- ( $10^{-3}$ )
$\mu$	Micro- ( $10^{-6}$ )
n	Nano- ( $10^{-9}$ )
p	Pico- ( $10^{-12}$ )

## SUMMARY

Transcytosis is the process by which macromolecules are transported across a polarized cell. It is one of the main methods of nutrient absorption from the blood stream as well as the only means past the blood brain barrier. Insight into the transcytic route has enormous medical potential where drug delivery methods stand to be significantly optimized. Despite the importance of this fundamental biological process, the mechanism of transcytosis is not well understood. Previously, fluorescence microscopy has allowed the tracking of fluorescently labeled low-density lipoprotein (LDL) intracellularly. However, this labeled LDL is not able to distinguish LDL particles undergoing transcytosis versus degradation. LDL is an ideal cargo for observing intracellular processes due to its vital role in transporting cholesterol for cell membrane fluidity. In order to differentiate transcytosis from degradation, I have produced two probes sensitive to degradation. The two probes are based on the principles of 1.) Förster resonance energy transfer (FRET) and 2.) fluorescence quenching. LDL degradation of the FRET-based or the fluorescence-quenching-based probe results in a significant increase in fluorescent activity. I have used several methods to assess the functionality of these probes including fluorescence measurements of detergent and enzyme degradations, SDS-PAGE analysis of degradations, and *in vivo* flow cytometry. Additionally, I have optimized the growth conditions for maintaining polarity in a cell line (MDCK) known to undergo transcytosis. The time and location of LDL degradation in a cell can be resolved through the use of these probes. Future work includes single-particle tracking of LDL as

it is being degraded versus actively transcytosing across a cell layer. This process is critical to understanding transcytosis as well as LDL regulation in the human body.

# CHAPTER 1

## INTRODUCTION

Transcytosis is the process by which macromolecules are transported across a polarized cell. It is a fundamental practice of all multicellular organisms as nutrient cargo needs to be distributed through many cell layers. Cells that undergo transcytosis regulate how much cargo is retained and degraded for individual cell use and how much is transported across to underlying tissues. The mechanism by which cells sort cargo between these pathways as well as efficiently transport cargo-containing vesicles across the length of the cell remains poorly characterized. In addition to determining how such regulation is achieved, understanding the transcytic route would have an extreme impact in pharmaceutical design; drugs could be optimized to enter the transcytic rather than the degradative route in cells. Additionally, transcytosis is the only method of entry past the blood brain barrier into the central nervous system. The blood brain barrier represents one of the most highly regulated areas of cellular transport (1). Insight into how transcytic regulation is performed in the blood brain barrier would allow for treatment of central nervous system disorders, such as Alzheimer's and Parkinson's disease. Resolving transcytosis has the potential to portray the details of a characteristic multicellular organism process. Such knowledge can be directly applied to drug delivery design and metabolic intracellular regulation.

### Significance of Transcytosis

Transcytosis involves active transport of cargo in vesicles across a cell. This mechanism involves endocytosis from one distinct surface and exocytosis from another site. A classic example of transcytosis occurs in epithelial cells when macromolecules

are endocytosed from the blood vessel at the apical surface and exocytosed at the basolateral surface to the underlying tissues. This process was initially described for its role in the immune response, as immunoglobulin undergoes receptor-mediated transcytosis to pass through cell layers (2). Medically, transcytosis is the center of enormous research efforts that seek to take advantage of natural cell transporting mechanisms for better drug uptake and efficiency. Transcytosis is, however, critical for more than just transport, as it also exists to establish cell polarity and to deliver proteins to the apical surface. Transcytosis is a key feature of any polarized cell or multicellular organism. Despite being a major pathway for membrane trafficking the specific mechanism by which transcytosis occurs remains debated.

Previously, transcytosis was described as a unique and completely devoted pathway in the cell (2). It was hypothesized to involve a special transcytic endosome that traveled the entire cell and directly fused to the opposite membrane. It has recently been shown that transcytosis more likely occurs by a combination of endo- and exocytic processes (3). In this manner, cellular components used for non-transcytic transport processes are utilized. A limitation of both of these conclusions results from the manner of inferring verification by elimination of the alternative. This indirect approach is very useful, but as of yet, no spatio-temporal model of transcytosis has been verified directly.

The goal of this research was to design and test the functionality of two probes for the use of tracking LDL transcytosis in polarized cells. These probes are sensitive to their environment, and display a distinct increase in fluorescent activity when exposed to degrading enzymes. This change in fluorescent activity is based on two principles for the two respective probes: 1.) Förster resonance energy transfer (FRET) and 2.) quenching.

The two probes will visualize transcytosis by distinguishing LDL particles that are undergoing a competing process of degradation. These probes are capable of elucidating the spatial and temporal kinetics of LDL transcytosis. By determining how this process occurs, it will be possible to understand the fundamental biological question of how macromolecules are transported across a cell. Additionally, such knowledge will allow for massive progress in the field of drug delivery where the transcytic route could be recruited for drug transport to specific tissues.

### **LDL as a Model Transcytic Cargo**

Low-density lipoprotein (LDL) is an ideal cargo for studying transcytosis due to its medical significance as well as advantageous physical structure (4). LDL, though infamous for its role in atherosclerosis, is essential to cellular function (5-7). LDL is biologically significant because it is the primary transporter of cholesterol from the liver to the peripheral tissues. Cholesterol is required to maintain the fluidity of the cell membrane and influences all membrane signaling and transport mechanisms (6). Due to the cellular importance of LDL, it is often used as a form of cargo that is readily visualized after staining with common fluorescent dyes. In order to stain the LDL particle, dyes take advantage of general LDL morphology. The core of LDL consists of hydrophobic cholesteryl esters and triacylglycerides and is surrounded by a phospholipid monolayer with free-floating unesterified cholesterol. Apolipoprotein B100 on the surface of the particle is responsible for recognition of the LDL particle to cell surface receptors (8). Currently, no structure exists for apolipoprotein B100, and modeling experiments have determined that only two of seven domains are embedded in the LDL core (9). The remainder of the domains is estimated to rest on the phospholipid

monolayer and maintain particle integrity. LDL integrity is lost with cleavage of apolipoprotein B100.

LDL taken in by the cell can be transported across an epithelial cell layer to be distributed to underlying tissues, such as the endothelial cells that line blood vessels. It is a representative marker for visualizing transcytosis. Additionally, LDL can be actively degraded by a transporting cell for the cell's own personal use. The trafficking process for LDL begins after endocytosis from the blood stream by LDL receptors. As the LDL travels intracellularly in the maturing endosome the pH decreases and causes release of the receptor-bound LDL particle. Once within the lysosome, LDL degradation begins to occur within 30 minutes to 2 hours (10). The lysosomal enzyme initially responsible for this degradation is cathepsin D, an aspartic protease known to produce many high-weight molecular fragments indicative of intermediate LDL degradation (11). Further degradation of LDL in the lysosome requires other thiol proteases, chief of which is cathepsin B (11, 12). Cathepsin B is known to produce many low molecular weight bands characteristic of a more thorough and efficient protease (11, 12). Both of these enzymes appear to cleave at distinct sites; however, the sites for each enzyme are not consistent with a particular residue sequence (12).

#### **Previous Work on LDL Transcytosis.**

Much of the knowledge of LDL degradation and cellular events comes from isotopic studies of <sup>125</sup>I-labeled LDL and gel electrophoresis, where only bulk rates of degradation can be found at relatively long time scales. This method was one of the first employed for analysis of LDL degradation, and further studies characterizing LDL molecular interactions still rely on this classical technique (13). This method, however,

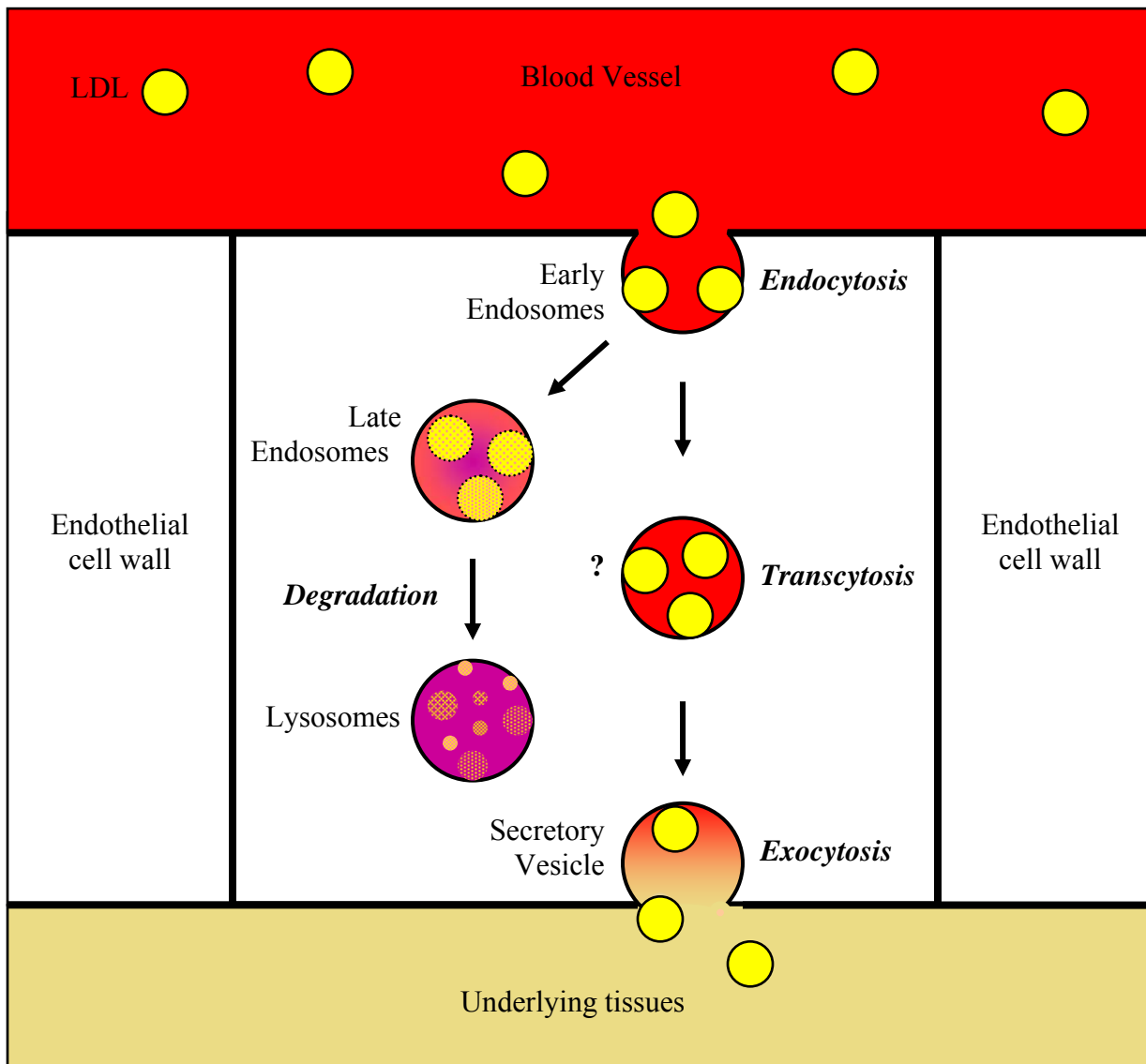


**Figure 1. Transcytic Route versus Degradative Route of Intracellular LDL.** This diagram depicts LDL intracellular pathways in the context of endothelial cells; this example is applicable to understanding the mechanism of transcytosis in the blood brain barrier. From the blood vessel, LDL binds to receptors on the endothelial cell surface. The LDL-receptors are endocytosed into vesicles known as early endosomes. From there, the most well-characterized pathway of LDL is degradation. LDL-containing early endosomes mature into late endosomes accompanied by a decrease in pH that disassociates the LDL cargo from its receptor, The LDL cargo is then exposed to proteases and lipases in the lysosome and enzymatic degradation of the particle occurs. Alternatively, LDL in endothelial cells or epithelial cells can be actively transported across the cell layer via transcytosis. The mechanism, vesicles, and active transporters are not well characterized in this process. After transcytosis, the LDL is then exocytosed from secretory vesicles to the underlying tissues.

observes the behavior of the apolipoprotein B100 and infers LDL interactions from this behavior. However, the distribution of cholesterol would be expected to change in the LDL particle as the transporter protein is cleaved, and tracking LDL degradation in this manner does not prove efficient. However, many assays are currently performed using fluorescently labeled LDL as an indicator of proper endocytosis and cellular functioning. Fluorescent tracking of molecules is highly sensitive and allows for dynamic, in vivo knowledge of interactions to be observed. One color labeled LDL is the current standard for observing LDL inter- and intra-cellular localization (14). Previous data demonstrates that this technique accurately portrays trafficking mechanisms of the LDL cargo (15). However, the one color labeled LDL does not yield any knowledge of the environment of the LDL cargo during transcytosis, such as a degrading scenario. The probes developed in this study can observe LDL degradation based on Förster resonance energy transfer (FRET, Figure 2) as well as fluorescence quenching. The lipophilic DiI and DiD were chosen due to their lipophilic nature; these particular fluorophores insert into the phospholipid monolayer of the LDL particle, representatively mimicking the behavior of cholesterol being carried in the same phospholipid monolayer. These fluorophores also fit the spectral overlap criteria for FRET where the emission overlap of DiI, the donor, overlaps with the absorption spectrum of DiD, the acceptor. This technique should yield data that better depicts the molecular interactions of cholesterol, which is the most biologically significant component of the LDL particle.

### **Principles of LDL Probe 1: Förster resonance energy transfer**

Based on the spherical nature of the LDL particle, and the non-linear decrease in surface area as volume decreases, it was hypothesized that degradation in an LDL particle

would be observed as a decrease in FRET signal (Figure 3). This relies on previous dynamic light scattering results that indicate smaller volume particles resulting from enzymatic degradation of apolipoprotein B100 (12). These smaller volume particles would have a larger surface area to volume ratio than the starting LDL particle, and the probability for FRET interactions should decrease with degradation. This lower probability of FRET interactions manifests itself as an increase in the donor emission to acceptor emission, as the fluorophores are not in close enough proximity to undergo energy transfer and the donor undergoes photon emission rather than energy transfer.

Only one group has attempted a similar protocol, G. Ouedraogo and R. Santus at the Institut de Recherche sur la Peau in Paris, France, when quantifying photolysis of lysosomal contents as inferred from a decrease in FRET (16). However, this FRET decrease was based on the light catalyzed destruction of the lysosome and its contents by the photosensitive antibiotic fluoroquinolones. FRET has not been used previously to observe the enzymatic degradation of LDL. Currently, the probes designed for this thesis undergo a decrease in FRET signal upon incubation of the LDL molecule with lysosomal and non-lysosomal enzymes, verifying the validity of the hypothesis.

### **Principles of LDL Probe 2: Fluorescence Quenching**

The sensitivity of the fluorescence quenching probe also relies on the three-dimensional nature of the LDL particle and the non-linear decrease in surface area as volume decreases. Normally, fluorescence is characterized by excitation from a light that causes photon absorption and emission of longer wavelength photons. Fluorescence is known as a form of radiative decay where the energy absorbed from the light in the form of a photon is re-emitted to the environment. When dyes are in very close proximity,

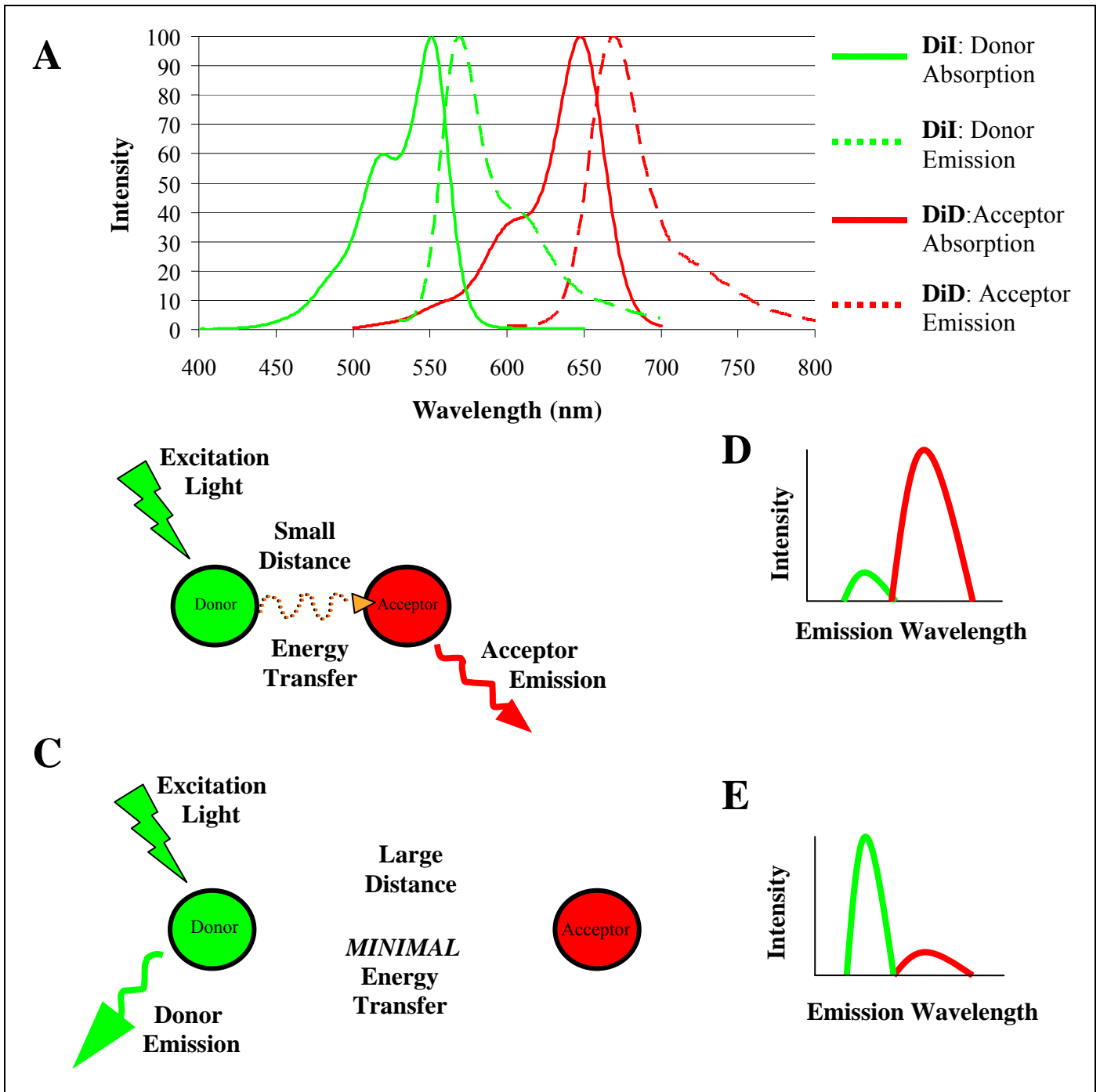


**Figure 2. Principles of FRET.** FRET is observed to occur when there is significant spectral overlap between the donor and acceptor dyes and a short distance between them. (A) The donor and acceptor dyes used in this experiment have spectral overlap. (B) FRET efficiency is higher when the donor and acceptor dyes are in close proximity; acceptor emission is observed even when using the donor excitation wavelength. (C) A larger distance between the donor and acceptor dye results in inefficient energy transfer; in this case, donor excitation results simply in donor emission. (D, E) The donor-acceptor distance scenarios can be observed in the ratio of donor emission to acceptor emission.

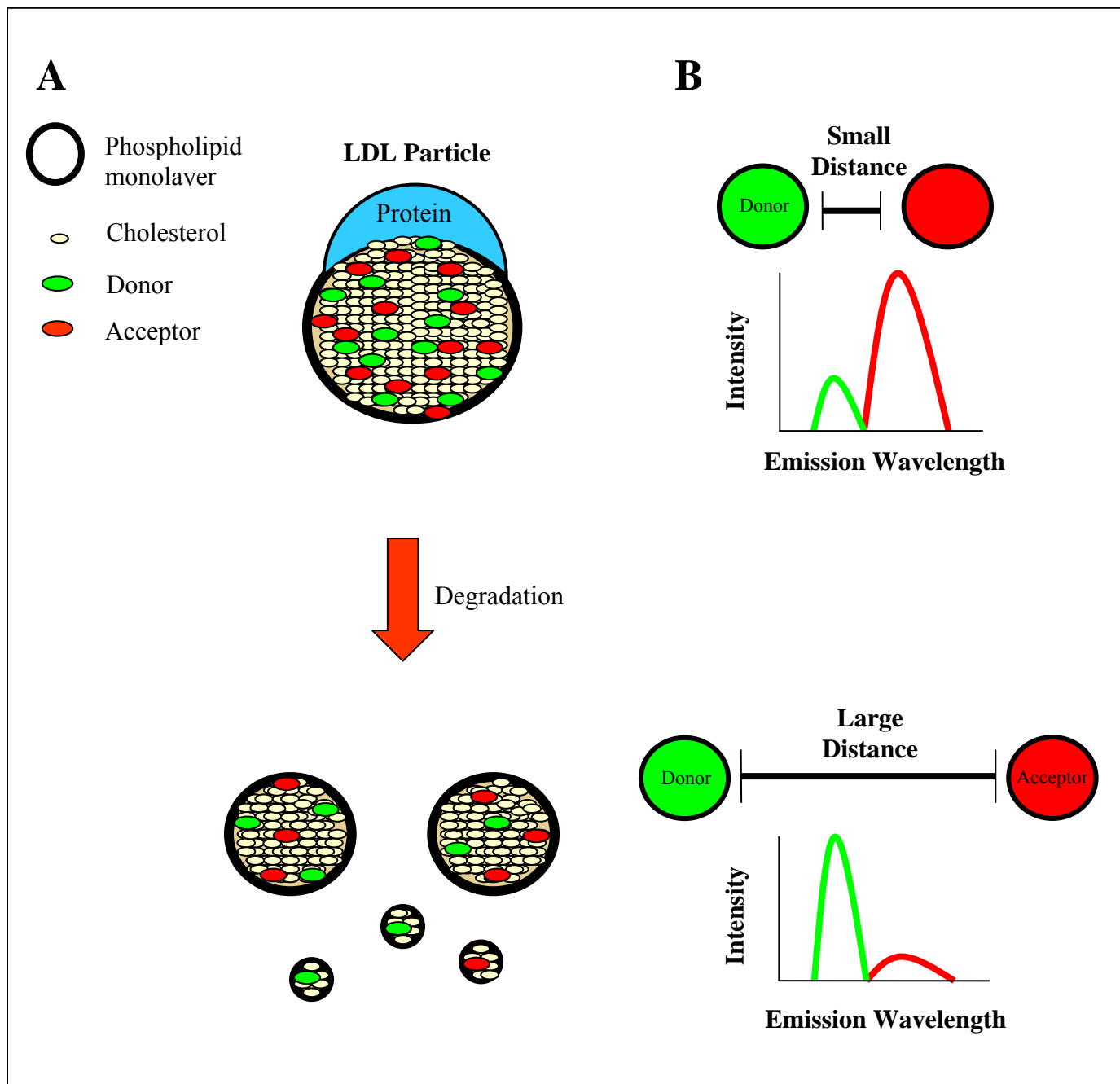


**Figure 3. Mechanism of FRET probe.** The lipophilic dyes embed themselves in the phospholipid monolayer that coats the LDL particle. (A) The intact LDL particle is characterized as having a lower surface area to volume ratio than the degradation products. This feature implies that dye molecules will have a higher probability of encountering each other and a higher FRET efficiency in the intact LDL particle. As degradation occurs the dye molecules will have a lower probability of encountering one another and donor emission will increase as acceptor emission decreases. (B) The average dye distance and corresponding fluorescence intensity graphs are shown to exemplify the data predicted during LDL degradation.

emission is not possible – an effect described as quenching. Instead, the energy is lost through non-radiative decay, such as transfer of energy to non-fluorophore molecules through collisions. Dyes at a high concentration are observed to increase significantly in fluorescence intensity as the concentration decreases to some determined threshold value. Fluorescence quenching is often taken advantage of in fluorescence microscopy. In terms of an LDL probe, fluorescence intensity is hypothesized to significantly increase upon degradation due to the large increase in the surface-to-volume ratio. This hypothesis was confirmed in this study, indicating that a fluorescence-quenching-based LDL probe would also be a useful tool for visualizing transcytosis. The fluorescence quenching technique has advantages over one-color labeling techniques, or even FRET, because an increase in fluorescence intensity is extremely less likely to occur than a decrease in fluorescence intensity. A decrease in fluorescence intensity can result from photobleaching of the fluorophore or the fluorophore moving out of the focus of the microscope; however, an increase in fluorescence intensity is rarely observed. A huge increase in the signal-to-noise ratio when tracking these fluorescence-quenching-based LDL probes should be gained.

### **Madin-Darby Canine Kidney Cells as a Model Cell Line for Transcytosis**

Transcytosis is a process characteristic of multicellular organisms (17). Nutrients require transport through cell layers in order to be distributed throughout tissues. The cells primarily responsible for transcytosis are epithelial cells; these cells line the internal side of all organs. Epithelial cells that line the blood vessels are a specialized form of epithelium known as endothelial cells (18). Transcytosis is critical for both nutrient distribution by the endothelial cells as well as macromolecule trafficking for the epithelial

cells that line the lumen of organs such as the liver, kidney, and gastrointestinal tract. For the endothelial cells, the polarized cell surfaces necessary for transcytosis are the apical and basolateral surface. The apical surface is defined as the surface that contacts the lumen of the blood vessel while the basolateral surface contacts the underlying tissues. For epithelial cells, the apical surface contacts the lumen of the organ while the basolateral surface absorbs macromolecules from underlying endothelial tissue.

Madin-Darby canine kidney cells (MDCK) were isolated from a female cocker spaniel in 1953 (19). These cells were initially harvested for the large electrical resistance produced when a current was applied across the monolayer. The characteristic high electrical resistance of these cells was a result of numerous tight-junctions that prevent paracellular movement, movement between cells, of molecules. Ions and other charged molecules are trapped on the distinct apical and basolateral sides of the cell monolayer inhibiting current flow and producing an electrical resistance comparable only to blood brain barrier cells. When paracellular transport of macromolecules is not possible, transcytosis becomes the only significant route of macromolecule trafficking; this is the case for the blood brain barrier cells and a similar situation for MDCK (20). MDCK cells are an excellent model system for studying transcytosis. These cells are easy to culture and ensure polarization. Protocols have already been developed in order to induce and verify proper polarization of the cell monolayer (21).

### **Applications of LDL Probes**

The results of the LDL probes establish an excellent technique for future *in vivo*, dynamic, single-molecule tracking of LDL during transcytosis. FRET and fluorescence quenching are poised to become a comprehensive labeling technique for cholesterol-

representative, dynamic, well-resolved imaging that confers structural characteristics of single particles. This is because traditional labeling methods, crystallization techniques, and standard protein or lipid protocols have shown poor to no yields for characterizing LDL structural qualities. The two LDL probes should serve as single-particle tracking tools for high resolution *in vivo* LDL localization and degradation. Intracellular movement of the LDL particle from the endosomes to the lysosomes, a poorly characterized process, can now be dynamically imaged and quantified using these probes. Transcytosis can also be clearly elucidated using these degradation-sensitive LDL probes. The goal of this research was to design and test the functionality of two probes for the use of tracking LDL transcytosis in polarized cells.

## CHAPTER 2

### EXPERIMENTAL METHODS

The probes were designed to have an increase in fluorescent activity upon degradation of the LDL particle. This initially required optimizing the fluorescent labeling of the LDL in order to get maximum FRET efficiency and quenching values with the intact LDL particle. An *in vitro* functionality test of the probe involved degradation via detergent and enzymes. An SDS-PAGE was used to confirm the results of the enzymatic degradation. An *in vivo* determination of probe functionality was performed via flow cytometry. The cell line known to undergo transcytosis was also fully characterized for proper polarization.

#### Materials

Human low density lipoprotein was obtained from Cappel (MP Biomedicals). The fluorescent, lipophilic fluorophores DiI (1,1'- dioctadecyl - 3,3,3',3'-tetramethylindocarbocyanine perchlorate) and DiD (1,1'- dioctadecyl-3,3,3',3'- tetramethylindocarbocyanine, 4-chlorobenzenesulfonate salt) were obtained from Molecular Probes (Invitrogen). These dyes were chosen due to their lipophilic nature and overlapping emission/absorption spectra. Lyophilized cathepsin B, cathepsin D, trypsin and chymotrypsin all came from Sigma-Aldrich. GE Healthcare illustra™ NAP-5 size exclusion chromatography columns were used to clean excess dye from the LDL particles. Cell lines were obtained from ATCC. All cell culture materials, including growth media, antibodies and fluid-phase markers, were obtained from Invitrogen except for the Transwell Filters (Corning).

## **Fluorescent Labeling of LDL**

LDL (250  $\mu\text{g}$ ) was incubated with various amounts of dye depending on the probe. For FRET, 110 dye particles per LDL particle were used in a ratio so that the molar absorptivities of each dye were equal between donor ( $\epsilon \sim 8000 \text{ L} \cdot \text{mol}^{-1} \cdot \text{cm}^{-1}$ ) and acceptor ( $\epsilon = 2036 \text{ L} \cdot \text{mol}^{-1} \cdot \text{cm}^{-1}$ ). This amounted to 82 acceptor molecules of DiD and 28 donor molecules of DiI per LDL particle. For the fluorescence quenching probe, the acceptor dye, DiD, was used at 28 molecules per LDL particle. Higher dye concentrations were observed to fully saturate the LDL particle as evidenced by a gross excess of dye during size exclusion chromatography. It was not possible to visually assess saturation of the lower dye concentrations in LDL. Different mixtures of dye were prepared in a DMSO stock solution. Various ratios were tested due to previous research emphasizing DiI having a magnitude greater absorbance and emission intensity than DiD (12). The incubation period involved gentle pipetting of the sample every ten minutes for an hour. Samples were then cleaned using a size exclusion chromatography column and measured for concentration by absorbance. When an absorbance concentration was not possible, concentration was estimated to be the determined average percent yield of the column (~75%).

## **Degradation of LDL Particle via Detergent and Enzymes**

Sorenson's buffer, consisting of 0.1 M phosphate pH 7.4, 1 mM EDTA, and 1 mM dithiothriitol was used for digest reactions at the physiological pH of blood. A 0.1 M sodium acetate buffer, 1 mM EDTA and 1 mM dithiothriitol, pH 5.5 was used for reactions at lysosomal pH. Detergent degradation was carried out under the two different pH values with 1% Triton-X 100 and a 30 minute incubation at 37°C. For all

degradations, 500  $\mu\text{g}/\text{mL}$  of LDL was used in a total volume of 100 $\mu\text{L}$ . Enzymatic degradation had an additional 40  $\mu\text{g}/\text{ml}$  of enzyme. Degradation with trypsin was at the physiological pH of the blood, 7.4; cathepsin B degradation was at the lysosomal pH 5.5. As a control, chymotrypsin and cathepsin D degradations were observed to yield similar results and only replicates of trypsin and cathepsin B were performed (data not shown)(22). The enzymatic degradations were incubated for 2 hours at 37°C and the reaction was then stored at 4°C. As a control, all degradation reactions were compared to a similarly incubated but non-detergent/enzyme exposed labeled LDL sample. Spectroscopic measurements were taken as soon as possible and small aliquots of the digest were taken for SDS-PAGE analysis.

#### **Visualization of Enzymatic Degradation via SDS-PAGE**

Gel electrophoresis was performed to confirm the degradation of LDL. Samples were prepared using a 1:1 ratio of Laemmli Sample buffer (1.5 M Tris-HCl, bromophenol blue, 15% glycerol, 5%  $\beta$ -mercaptoethanol) and boiled for 5 minutes prior to loading. An SDS-PAGE composed of 5 varying acrylamide bands (4, 8, 12, 16, 20% respectively) was prepared for electrophoresis in a Mini-Protean 3 gel electrophoresis system (Bio-Rad). High range and low range molecular weight markers from Bio-Rad were also used. The voltage was a constant 120 V run for one hour, and staining and destaining were performed overnight.

#### **Spectroscopic Measurements**

Absorbance measurements were taken in a Beckman Coulter DU® 800 spectrophotometer with a Beckman Coulter 50  $\mu\text{L}$  UV silica cuvette (path length: 10 mm, path width: 2.0 mm). Fluorescence emission measurements were taken in a Shimadzu

RF-5301 PC spectrofluorophotometer in a Hellma 50  $\mu$ L quartz cuvette (type no: 105.254-QS, light path: 3 mm). LDL concentration was determined at an absorbance of 271 nm. DiI, the FRET donor fluorophore, had a maximum absorbance at 554 nm, however, an excitation wavelength of 530 nm was used to avoid exciting the acceptor dye. The maximum emission for DiI was 580 nm. DiD maximum absorbance occurred at 648 nm, but an excitation wavelength of 630 nm was used to better resolve the maximum emission at 670 nm. When lipids were absent, DiD was verified to be non-fluorescent while DiI was determined to be weakly fluorescent (data not shown). FRET calculations were made by comparing donor emission at 580 nm to acceptor emission at 670 nm. An increase in FRET signal would be seen as a decrease in the ratio of donor emission to acceptor emission. A change in quenching was observed as an increase in fluorescence intensity after degradation and these measurements often required multiple dilutions to prevent detector saturation. The presence of the fluorophores was verified throughout the experiment by taking the absorbance of all solutions.

### **Cell Culture**

MDCK type II cells (ATCC CCL-34<sup>TM</sup>) were propagated in Eagle's Minimal Essential Medium with 10% (v/v) fetal bovine serum in a 5% CO<sub>2</sub> atmosphere at 37°C. Cells had the medium replaced daily and were split every 3-4 days. In order to break up the tight monolayer, splitting involved rinsing once and incubating for approximately 15 minutes with a trypsin-EDTA mixture (2.5 g/L trypsin, 0.38 g/L EDTA·4Na, 60.000 g/L NaCl, 4.000 g/L KCl, 0.600 g/L KH<sub>2</sub>PO<sub>4</sub>, 0.479 g/L Na<sub>2</sub>HPO<sub>4</sub>, 0.100 g/L Sodium-salt phenol red). For use in transcytic assays, cells were seeded on 0.4  $\mu$ m pore-sized Corning Transwell-clear filters (12 and 24 mm diameter for 12 and 6-well plates

respectively) so that confluence was reached within 2 days. Another cell line, BS-C-1 (ATCC CCL-26<sup>TM</sup>), was used for simple flow cytometry experiments. The BS-C-1 cells were grown under similar conditions as MDCK without the Transwell filters.

### **Determining MDCK Polarization**

Kidney epithelial cells require polarization of the cell surface before transcytosis can properly occur (10, 23-27). This involves the formation of distinct apical and basolateral domains that are separated by the numerous tight junctions. Three methods of assaying MDCK polarization were used. Cells were grown for at least 2 days before measurements. A Millipore Millicell transepithelial resistance (TEER) device was used to measure characteristic TEER values of the cell monolayer (23, 24, 28, 29). Polarized tight junction formation also inhibits paracellular leakage (30). Paracellular leakage can be detected with a monolayer integrity test (24). This measures the monolayer rejection of rhodamine-dextran (tetra-methyl-rhodamine), a fluid-phase marker, when cells are grown on the Transwell filters. Additionally, immunostaining via FITC-conjugated- $\alpha$ -tubulin was used to look for characteristic reorganization of the microtubule cytoskeleton (24). This assay involved seeding a glass-well plate in a similar method as seeding the Transwell filters.

### **Testing LDL Quenching Probe *in vivo* by Flow Cytometry**

An *in vivo* analysis of probe functionality used a flow cytometer (Becton Dickinson FACS Vantage SE). BS-C-1 cells were grown to confluence for 5 days before LDL labeling began. The cells were incubated on ice for 10 minutes, and then incubated an additional 10 minutes on ice with 14.3  $\mu$ g of LDL labeled with the quenching probe in fresh cold medium. The cells were then rinsed and incubated for the designated time.

Cells were rinsed twice with Liebovitz medium before collecting for flow cytometry via scraping. An APC-CY5 filter was used for the quenching LDL probe.

## CHAPTER 3

### RESULTS

#### **Determination of Labeled LDL Concentration**

A standard curve was generated in order to determine concentrations of the column-cleaned labeled LDL to use in the digests (Figure 4A). It was found that the dye altered the absorbance reading in the 280 nm region of the LDL spectrum (Figure 4B). This discovery indicated that absorbance of the labeled LDL particle was not a reliable means of assessing concentration. Instead, estimates of column-cleaned labeled LDL concentration were based on the average percent yield of the columns. All degradations reactions used consistent volumes - 100  $\mu$ L.

#### ***In vitro* Detergent Degradation of LDL Probes**

As a control, the LDL probes were fully dissolved using Triton-X 100. Triton-X 100 is a non-ionic surfactant whose hydrophobic alkyl chain inserts into the LDL particle core. Incubation of LDL with Triton-X 100 dissolves the intact LDL particle via the numerous competing hydrophobic interactions with the amphipathic detergent Triton-X 100; this has previously been shown to abolish FRET efficiency (16). All degradation assays were run alongside a sample of non-detergent exposed fluorescently labeled LDL to control for temperature and pH effects. The resulting percent change after degradation was normalized to the control sample.

#### **Detergent Degradation of Probe 1: FRET Probe**

Incubation at 37°C for 30 minutes in the absence of detergent and at either tested pH was found to increase FRET efficiency approximately 15% (data not shown). This result was most likely due to increasing movement of the lipophilic dyes on the surface

and the probability of them encountering one another. The detergent-incubated dyes were normalized to the non-detergent-exposed FRET probes. As predicted, detergent exposure reduced FRET efficiency of the FRET probes. Due to the decrease in efficiency, the ratio of FRET shifts from a higher acceptor emission to a higher donor emission. This was observed as an increase in the FRET ratio above the defined pre-degradation value of 100% (Figure 5A). The percent changes 142% and 240% were observed at a pH of 7 and 5 respectively, in the FRET ratio. A 99% greater change was observed at pH 5 than pH 7 indicating enhanced degradation of LDL under lysosomal pH.

#### **Detergent Degradation of Probe 2: Quenching Probe**

The fluorescence quenching based probe was similarly tested for functionality. The non-detergent exposed control was observed to have an approximately 32% increase in fluorescence intensity at both pH values after the timed incubation (data not shown). This was in contrast to the enormous response for the detergent exposed quenching probe; fluorescence intensity changed over a magnitude (Figure 5B). For a pH of 7, 1900% percent change in the fluorescent intensity was observed. At a pH of 5, 2390% increase in the fluorescence intensity was observed. The lysosomal pH 5 had a percent change 488% greater than the fluorescence intensity change observed at a pH of 7.

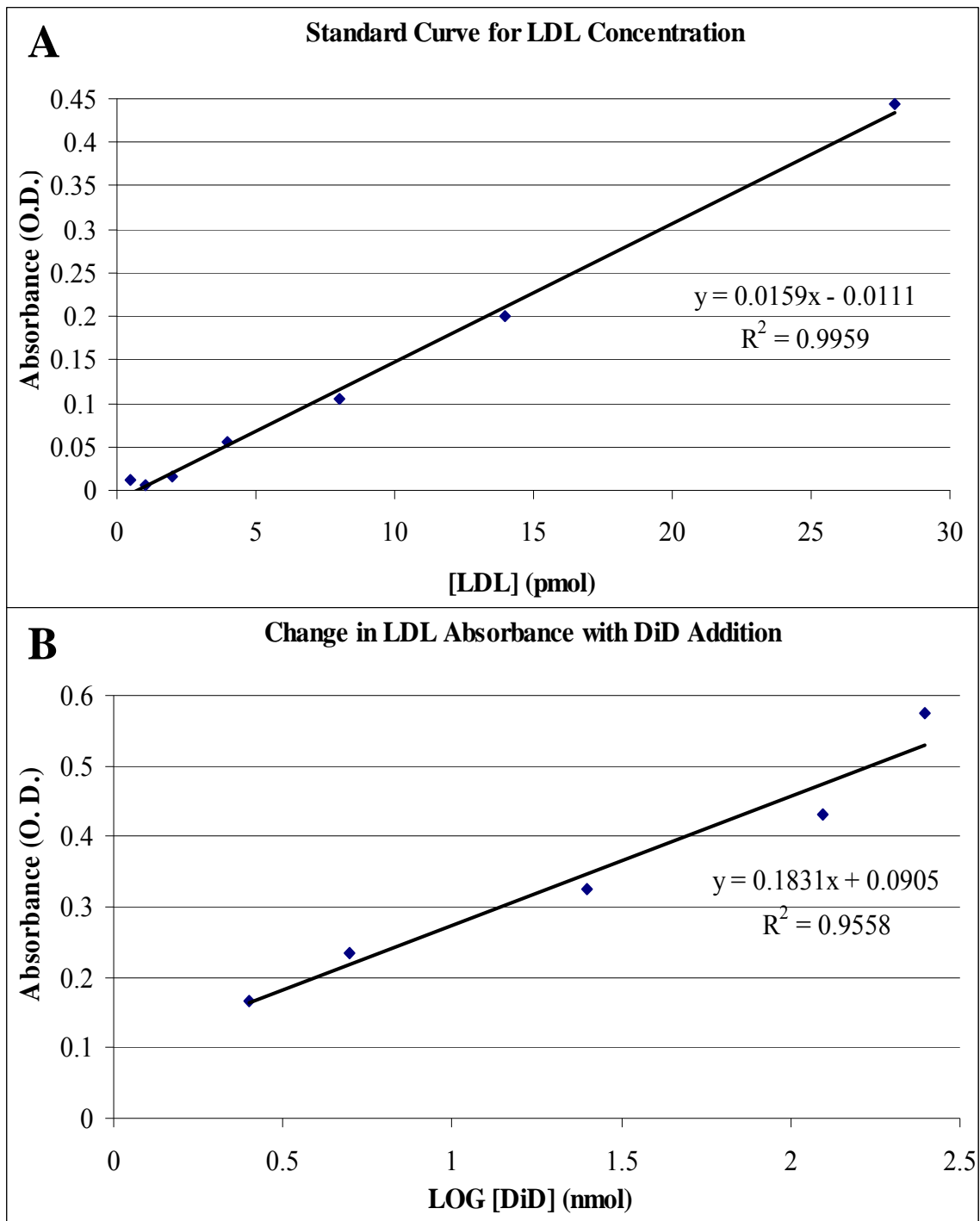


**Figure 4. LDL Absorbance at 271 nm.** Absorbance at 271 nm was affected by LDL concentration as well as DiD dye concentration. (A) A calibration curve shows the linear change in absorbance as LDL concentration was increased. (B) LDL absorbance was also observed to have a linear logarithmic change as DiD was titrated into the sample. LDL concentration was held constant at 7.5 nmol.

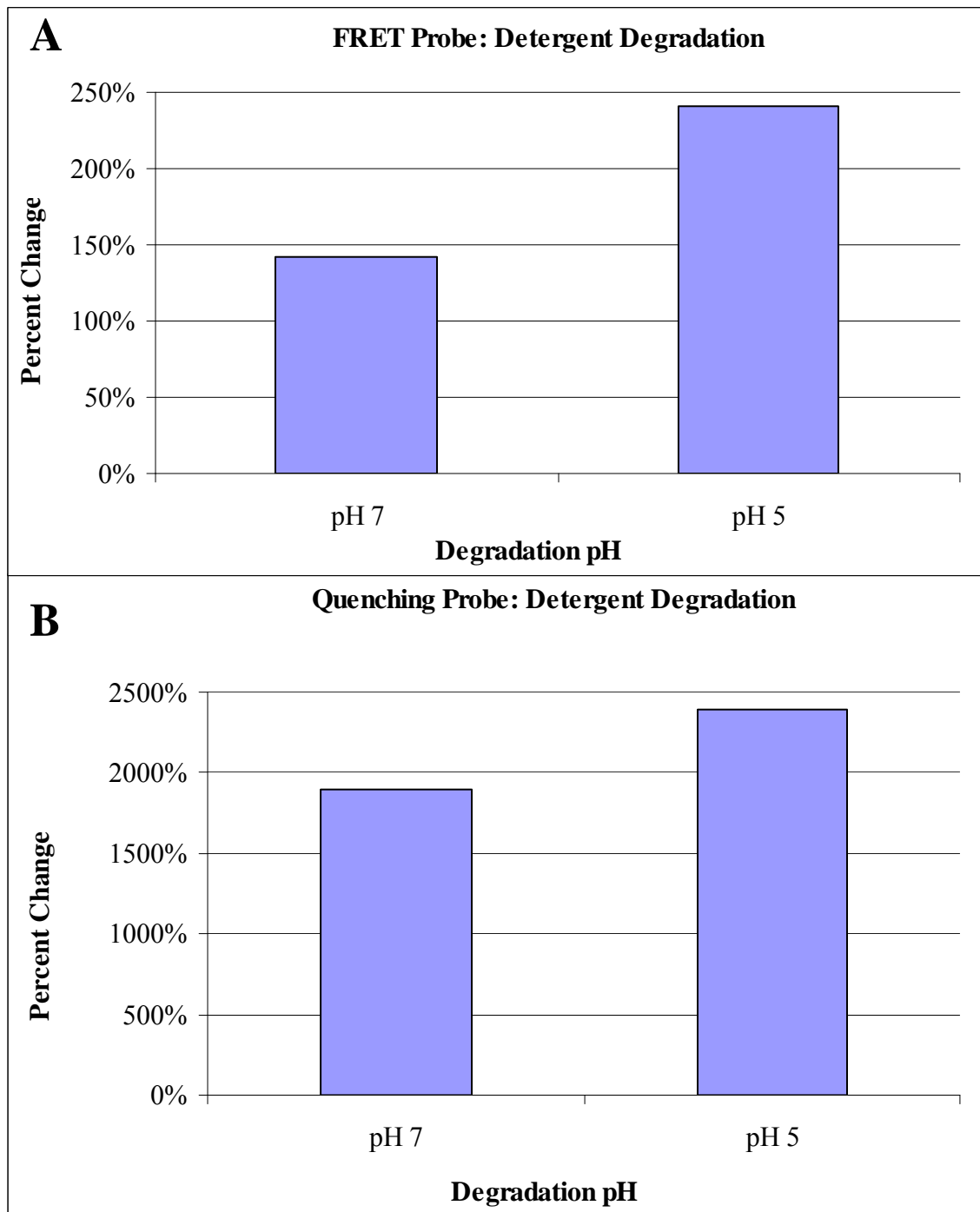


**Figure 5. *In vitro* Detergent Degradation of Probes.** Triton-X 100 was used to dissolve the LDL particles and sensitivity of the probes was measured as a percent change from starting values (100%). (A) The FRET probe was observed to have an increase in the donor to acceptor emission ratio after degradation. (B) The quenching probe was observed to have an enormous increase in fluorescence intensity after degradation.

### ***In vitro* Enzymatic Degradation of LDL Probes**

The probes were then analyzed for functionality in an *in vitro* enzyme digest. Trypsin was chosen as a general control enzyme commonly used in degradation assays. It performs ideally at a higher pH such as the pH of the bloodstream at 7.4. Cathepsin B is a lysosomal thiol protease normally involved in LDL degradation within the lysosome. Cathepsin B works ideally at the pH of the lysosome, 5.5. The samples were excited at the donor excitation wavelength, 530 nm, and emission was measured at 580 nm for the donor and 670 for the acceptor.

#### **Enzymatic Degradation of Probe 1: FRET Probe**

The FRET probe was observed to have an increase in the donor to acceptor emission ratio after cathepsin B treatment (Figure 6A). After trypsin treatment, there was a decrease in the donor to acceptor emission ratio.

#### **Enzymatic Degradation of Probe 2: Quenching Probe**

The quenching probe was observed to have minimal increases after enzyme incubation.

#### **Visualization of Enzymatic Degradation via SDS-PAGE**

After digestion, aliquots of the reaction sample were visualized on SDS-PAGE and degradation was confirmed (Figure 7). LDL incubated in the absence of enzyme was observed to have 2-3 bands above 200 kDa, which previous data explains as apolipoprotein B or possibly E sometimes exiting the LDL particle.<sup>3,4</sup> The enzymes displayed distinct banding patterns with trypsin producing the smallest products (Figure 7B). Bands were observed to become linearly fainter in the lanes containing increasing concentrations of dye in the LDL particle.

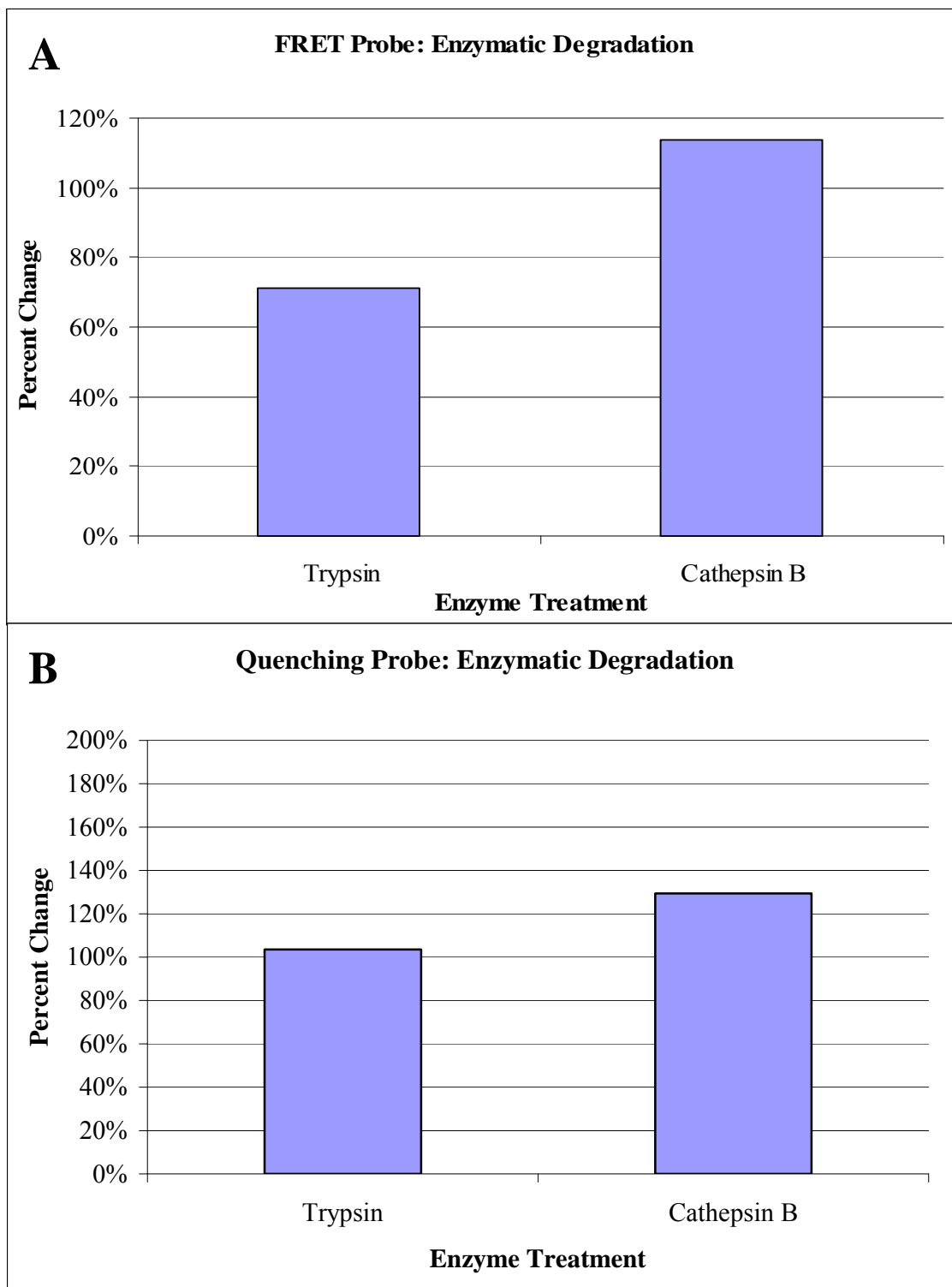


**Figure 6. *In vitro* Enzymatic Degradation of Probes.** LDL is normally broken down by lysosomal enzymes so an *in vitro* single enzyme degradation was performed to test probe functionality. Functionality of the probes was measured as a percent change from starting values (100%). (A) The FRET probe was observed to have an inconsistent response to enzyme degradation. The quenching probe was observed to have a minimal increase in fluorescence intensity after degradation (B).

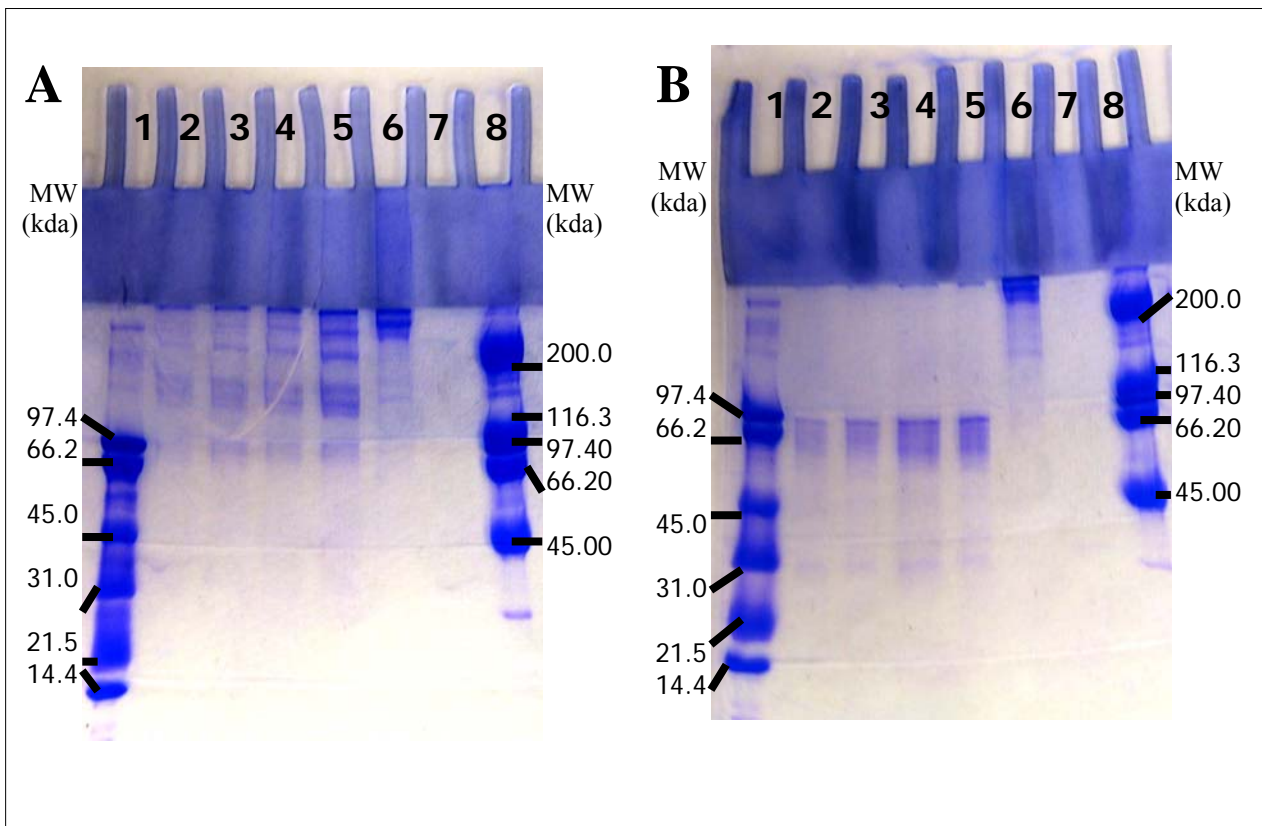


**Figure 7. Visualization of FRET Probe Enzymatic Degradation via SDS-PAGE.** Degradation was confirmed by SDS-PAGE analysis of the reaction mixture. (A) Cathepsin B was the enzyme used for this gel. (B) Trypsin was the enzyme used for this gel. Lanes 1 and 8 contained molecular weight standards. Lanes 2-6 contained LDL (10 µg) with a decreasing concentration of FRET dyes (250, 250, 25, 0, and 0 nmol of dye). The reaction mixtures in lanes 2-5 also contained enzyme (0.03 µg) during incubation. Lane 7 was a reaction mixture consisting of only enzyme (0.03 µg) to ensure an absence of enzyme contribution to band intensity. A.) Enzyme for digestion was cathepsin B. B.) Enzyme for digestion was trypsin.

### Testing LDL Quenching Probe *in vivo* via Flow Cytometry

A flow cytometer was used to rapidly measure the fluorescent intensity of numerous cells (20,000 cells). A control sample with no LDL probe was used to define the autofluorescence as 98% of the control population. The remaining 2% of the population of interest was defined as being significantly fluorescent and for the remaining fluorescently labeled cells, the % population above the threshold autofluorescence were

counted. The fluorescence mean intensity is a relative comparison of the fluorescence intensity above the autofluorescence of the cell. A zero time point during the LDL incubation represents the fluorescently labeled LDL resting on the cell surface. This LDL was cold-bound and should not have been exposed to any degrading conditions. The LDL probe was observed to contribute a 10.0% greater increase to the fluorescence (Table 1). At 2 hours, a 92% increase in fluorescence intensity indicated degradation of the probes. At 24 hours, mean intensity began to decrease to 93%, possibly indicating degradation of the fluorescent dyes themselves.

<b>Table 1. <i>In vivo</i> Quenching Probe Degradation via Flow Cytometry</b>		
<b>Probe Incubation Time</b>	<b>% Population with Significant Fluorescence Intensity</b>	<b>Fluorescence Mean Intensity</b>
t = 0	10%	128
t = 2 hr	92%	474
t = 24 hr	93%	337

### **Assaying Polarization of MDCK Monolayer**

Millipore Millicell transepithelial resistance (TEER) device was used to measure characteristic TEER values of the cell monolayer (Figure 8). TEER values are observed to be very high (~500 ohms\* cm<sup>2</sup>) indicating that tight junctions have formed very tightly regardless of seeding density. A seeding volume of 0.50 mL was determined to be ideal for MDCK polarization. Another assay for tight junction formation is the rejection of the fluid-phase marker rhodamine dextran. MDCK monolayer cells were observed to reject almost all of the fluid phase marker (Table 1). Additionally, immunostaining via FITC-

conjugated- $\alpha$ -tubulin was used to look for characteristic reorganization of the microtubule cytoskeleton (Figure 9). A monolayer integrity test using rhodamine-dextran was also used to assess integrity of the tight junctions (Table 1). All the results indicate polarization of the MDCK monolayer as expected.

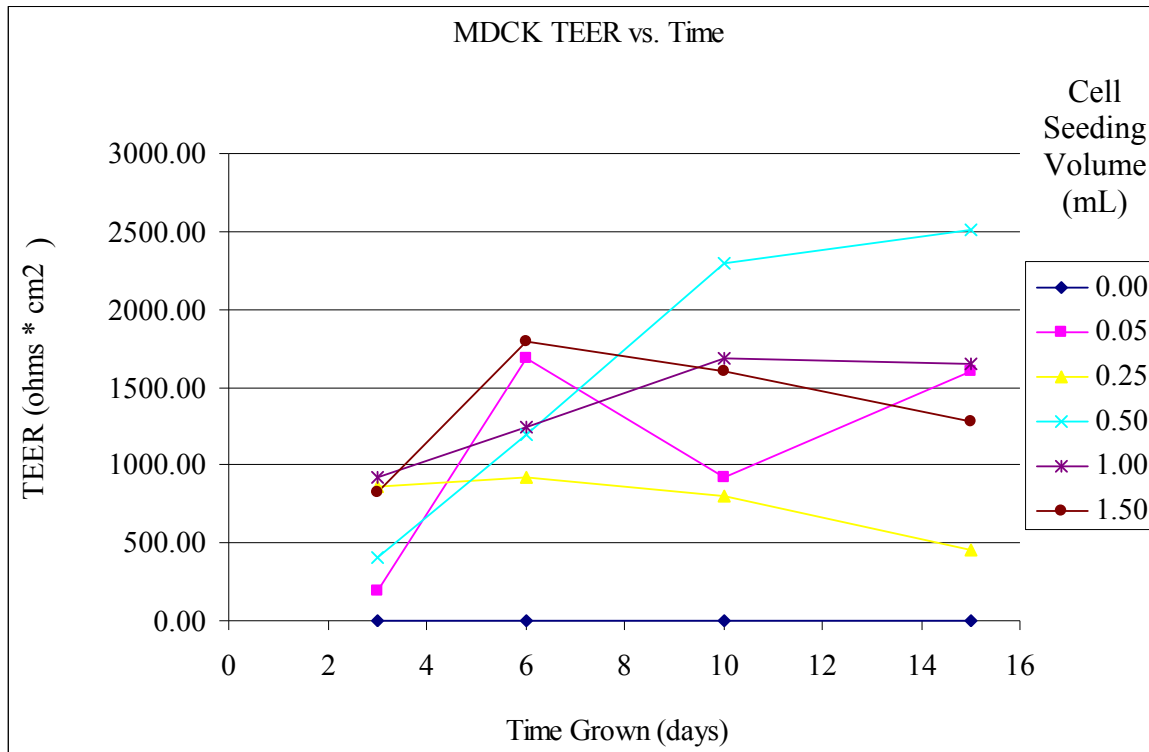


**Figure 8. MDCK TEER values over Time.** As MDCK forms a tight monolayer with numerous tight junctions, TEER values are observed to initially increase before plateauing.

Table 2. Rhodamine-Dextran Rejection Assay	
Cell Seeding Volume (mL)	Average % Rejected
0.1	97.27%
1.0	99.95%

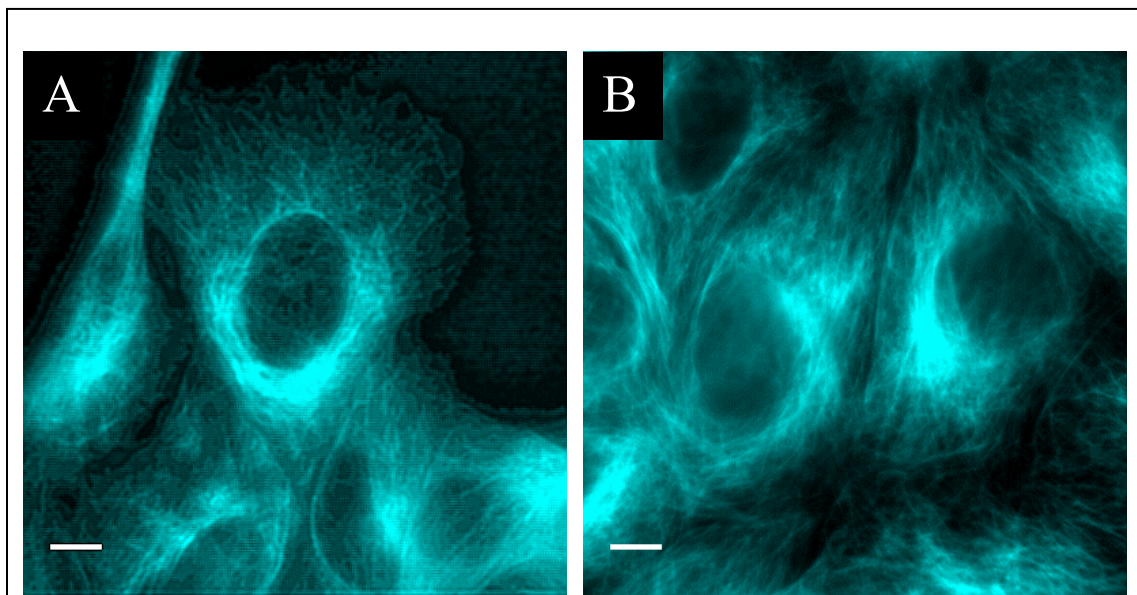


**Figure 9. Images of Microtubule Reorganization after Polarization.** Polarized cells have been observed to undergo microtubule reorganization. (A) In an unpolarized cell, microtubules are aligned horizontally to the cell surface and observed as long linear stretches of microtubules. (B) In polarized cells, microtubules align themselves vertically and are viewed as short small specks of microtubule complex. Scale bar is to 10  $\mu\text{m}$ .

## CHAPTER 4

### DISCUSSION

The purpose of the research was to investigate the functionality of two fluorescent LDL probes. These probes were designed to be sensitive to intracellular degradation so that degradative pathways and transcytic pathways could be differentiated. The biological significance of LDL in cholesterol transport has yielded interest in LDL as a cargo. Additionally, insight into how transcytosis occurs has enormous medical potential. Sensitive fluorescent techniques, such as FRET and fluorescence quenching, are poised to become a comprehensive labeling technique for cholesterol-representative, dynamic, well-resolved imaging that confers structural characteristics of single particles.

The detergent degradation indicated high probe functionality. However, the *in vitro* enzymatic degradation of the LDL probes was not consistent with detergent degradation or *in vivo* flow cytometry results. This is hypothesized to be an artifact of artificial degradation of the LDL. Physiologically, LDL would be exposed to numerous proteases that act in a concerted effort to degrade the particle. The single enzyme experiments are far removed from the normal degradation of LDL, and increasing concentration of the enzyme still displayed a saturating amount of enzyme activity (data not shown). Flow cytometry depicted the *in vivo* functionality of this probe.

The change in fluorescent activity for both probes should be easily tracked during *in vivo* imaging. Additionally, further characterization of the LDL particles' mass and size distribution through dynamic light scattering and electron microscopy would allow for a more quantitative description of how FRET and fluorescence quenching mechanisms rely on a changing surface area to volume ratio. Other results indicate a

much more complex interaction of the dyes in the LDL environment. Much of the data provides evidence that the dye may be altering normal LDL interactions, or that LDL interactions are altering dye spectral properties. The implications for this discovery are substantial since similarly 1-color labeled LDL is the current standard for observing LDL inter- and intra-cellular localization (13). Previous data demonstrates that labeled LDL is inhibited and displaced by a competing concentration of unlabeled LDL when observing cell surface interactions (14).

This concern was first encountered when the dye was found to alter the absorbance peak of the protein at 271 nm. An initial hypothesis involved the fluorophore inducing protein conformational changes and changing the local environment of apolipoprotein B100's aromatic groups. However, no change in banding pattern between labeled and unlabeled LDL was observed after chymotrypsin degradation, showing that vulnerability of the aromatic residues was not significantly impacted by the dye (data not shown). Additionally, all of the enzymes behaved consistently between the labeled and unlabeled dyes, indicating that overall protein conformation was consistent enough for proper degradation.

Although the dye and the LDL particle seem to have indiscernible interactions, observation of LDL degradation via FRET and fluorescence quenching was still possible. Under the determined concentration, FRET donor emission was significantly increased while acceptor emission decreased. Similarly, over a magnitude increase in fluorescence intensity was observed for the fluorescence quenching probe. These probes have proven themselves in a control detergent degradation assay as well as *in vivo* flow cytometry experiments.



## CHAPTER 5

### CONCLUSION

Future work will involve further characterizing the *in vivo* applications of the two probes. Flow cytometry experiments that measure probe functionality require a finer range of time points. This will allow the degradation of the fluorescent probes to be tracked *in vivo* in a bulk cell sample. Additionally, specific cell behavior-altering reagents will be able to verify the location of the probe. This includes using wortmannin to inhibit endosome-lysosome fusion in order to ensure degradation is occurring in the lysosomes. Colocalization experiments with various vesicles can accurately identify subcellular regions of LDL incubation. Single-particle tracking of LDL-containing vesicles will visualize temporal-spatial information on LDL degradation and transcytosis. This experiment determined protocols for verifying MDCK polarization indicating a ready model system for single-particle tracking of the fluorescent probes. Intracellular movement of the LDL particle from the endosomes to the lysosomes, a poorly characterized process, can now be dynamically imaged and quantified using these probes. This will allow for the mechanism of transcytosis to be investigated.

This study has verified the hypothesis that both the FRET and fluorescence quenching probes respond significantly during LDL degradation. As a result, the probes should be able to discern transcytosing LDL from degrading LDL; this function will be useful for elucidating the process of transcytosis. Understanding the fundamental basics of transcytosis will aid in drug delivery especially in transcytosis-exclusive cells such as in the blood brain barrier.

## REFERENCES

1. Pardridge, W. M. (1998) CNS Drug Design Based on Principles of Blood-Brain Barrier Transport, *Journal of Neurochemistry* 70, 1781.
2. Apodaca, G., Katz, L. A., and Mostov, K. E. (1994) Receptor-mediated transcytosis of IgA in MDCK cells is via apical recycling endosomes, *J. Cell Biol.* 125, 67-86.
3. Rojas, R., and Apodaca, G. (2002) Immunoglobulin transport across polarized epithelial cells, *Nature Reviews. Molecular Cell Biology* 3, 944-955.
4. Dehouck, B., Fenart, L., Dehouck, M. P., Pierce, A., Torpier, G., and Cecchelli, R. (1997) A New Function for the LDL Receptor: Transcytosis of LDL across the Blood-Brain Barrier, *The Journal of Cell Biology* 138, 877-889.
5. Brown, D. A., and London, E. (1998) FUNCTIONS OF LIPID RAFTS IN BIOLOGICAL MEMBRANES, *Annual Reviews in Cell and Developmental Biology* 14, 111-136.
6. Ohvo-Rekilä, H., Ramstedt, B., Leppimäki, P., and Peter Slotte, J. (2002) Cholesterol interactions with phospholipids in membranes, *Progress in Lipid Research* 41, 66-97.
7. Sullivan, D. (1994) Cholesterol and non-cardiovascular disease: basic science, *Internal Medicine Journal* 24, 92-97.
8. Houlston, R. S., Turner, P. R., Lewis, B., and Humphries, S. E. (1990) Genetic Epidemiology of Differences in Low-Density Lipoprotein (LDL) Cholesterol Concentration: Possible Involvement of, *Genetic Epidemiology* 7, 199-210.
9. Krisko, A., and Etchebest, C. (2007) Theoretical Model of Human Apolipoprotein B100 Tertiary Structure, *PROTEINS: Structure, Function, and Bioinformatics* 66, 342-358.
10. Maxfield, F. R., and Mondal, M. (2006) Sterol and lipid trafficking in mammalian cells, *Biochem. Soc. Trans.* 34, 335-339.
11. van der Westhuyzen, D. R., Gevers, W., and Coetzee, G. A. (1980) Cathepsin-D-dependent initiation of the hydrolysis by lysosomal enzymes of apoprotein B from low-density lipoproteins, *European Journal Of Biochemistry / FEBS* 112, 153-160.
12. Linke, M., Gordon, R. E., Brillard, M. I., Lecaille, F., Lalmanach, G., and BrÄ¶mme, D. (2006) Degradation of apolipoprotein B-100 by lysosomal cysteine cathepsins, *Biological Chemistry* 387, 1295-1303.

13. Ostlund Jr., R. E., Pflieger, B., and Schonfeld, G. (1979) Role of Microtubules in Low Density Lipoprotein Processing by Cultured Cells, *Journal of Clinical Investigation* 63, 75-84.
14. Wang, M.-D., Kiss, R. S., Franklin, V., McBride, H. M., Whitman, S. C., and Marcel, Y. L. (2007) Different cellular traffic of LDL-cholesterol and acetylated LDL-cholesterol leads to distinct reverse cholesterol transport pathways, *J. Lipid Res.* 48, 633-645.
15. Barak, L. S., and Webb, W. W. (1981) Fluorescent low density lipoprotein for observation of dynamics of individual receptor complexes on cultured human fibroblasts, *J. Cell Biol.* 90, 595-604.
16. Ouedraogo, G., Morliere, P., Maziere, C., Maziere, J. C., and Santus, R. (2000) Alteration of the Endocytic Pathway by Photosensitization with Fluoroquinolones, *Photochemistry and Photobiology* 72, 458-463.
17. Tuma, P. L., and Hubbard, A. (2003) Transcytosis: Crossing Cellular Barriers, *Physiological Reviews* 83, 871-932.
18. Di Pasquale, G., and Chiorini, J. A. (2006) AAV Transcytosis through Barrier Epithelia and Endothelium, *Molecular Therapy* 13, 506-516.
19. Stulberg, C. S., Coriell, L. L., Kniazeff, A. J., and Shannon, J. E. (1970) The animal cell culture collection, *In Vitro Cellular & Developmental Biology-Plant* 5, 1-16.
20. Rubin, L. L., and Staddon, J. M. (1999) THE CELL BIOLOGY OF THE BLOOD-BRAIN BARRIER, *Annual Reviews in Neuroscience* 22, 11-28.
21. Balcarova-Ständer, J., Pfeiffer, S. E., Fuller, S. D., and Simons, K. (1984) Development of cell surface polarity in the epithelial Madin-Darby canine kidney (MDCK) cell line, *The EMBO Journal* 3, 2687.
22. Hakala, J. K., Oksjoki, R., Laine, P., Du, H., Grabowski, G. A., Kovanen, P. T., and Pentikainen, M. O. (2003) Lysosomal Enzymes Are Released From Cultured Human Macrophages, Hydrolyze LDL In Vitro, and Are Present Extracellularly in Human Atherosclerotic Lesions, *Arterioscler Thromb Vasc Biol* 23, 1430-1436.
23. Parton, R. G., Prydz, K., Bomsel, M., Simons, K., and Griffiths, G. (1989) Meeting of the apical and basolateral endocytic pathways of the Madin- Darby canine kidney cell in late endosomes, *J. Cell Biol.* 109, 3259-3272.

24. Bomsel, M., Prydz, K., Parton, R. G., Gruenberg, J., and Simons, K. (1989) Endocytosis in filter-grown Madin-Darby canine kidney cells, *J. Cell Biol.* *109*, 3243-3258.
25. Ang, A. L., Folsch, H., Koivisto, U.-M., Pypaert, M., and Mellman, I. (2003) The Rab8 GTPase selectively regulates AP-1B-dependent basolateral transport in polarized Madin-Darby canine kidney cells, *J. Cell Biol.* *163*, 339-350.
26. Barocchi, M. A., Ko, A. I., Reis, M. G., McDonald, K. L., and Riley, L. W. (2002) Rapid Translocation of Polarized MDCK Cell Monolayers by *Leptospira interrogans*, an Invasive but Nonintracellular Pathogen, *Infect. Immun.* *70*, 6926-6932.
27. Brandli, A. W., Parton, R. G., and Simons, K. (1990) Transcytosis in MDCK cells: identification of glycoproteins transported bidirectionally between both plasma membrane domains, *J. Cell Biol.* *111*, 2909-2921.
28. McNeil, E., Capaldo, C. T., and Macara, I. G. (2006) Zonula Occludens-1 Function in the Assembly of Tight Junctions in Madin-Darby Canine Kidney Epithelial Cells, *Mol. Biol. Cell* *17*, 1922-1932.
29. Staddon, J. M., Herrenknecht, K., Smales, C., and Rubin, L. L. (1995) Evidence that tyrosine phosphorylation may increase tight junction permeability, *J Cell Sci* *108*, 609-619.
30. Pfeffer, S. R., Leung, S. M., Ruiz, W. G., and Apodaca, G. (2000) Sorting of Membrane and Fluid at the Apical Pole of Polarized Madin-Darby Canine Kidney Cells, *Molecular Biology of the Cell* *11*, 2131-2150.